Available online at www.sciencedirect.com
SCIENCE DIRECT®

Journal of the European Ceramic Society 23 (2003) 2737–2740
www.elsevier.com/locate/jeurceramsoc

Oxygen vacancies at Ni/c-ZrO_2 interfaces

J.I. Beltrán, S. Gallego, J. Cerdá, M.C. Muñoz*

Instituto de Ciencia de Materiales de Madrid, Consejo Superior de Investigaciones Científicas, Cantoblanco, 28049 Madrid, Spain

Abstract

The interaction between Ni(001) and cubic-ZrO_2(001) surfaces is investigated, focusing on the role of the O vacancies that actually exist in the c-ZrO_2 phase stabilized at room temperature. Ab-initio calculations of the electronic charge distribution are performed, allowing full relaxation of the atomic positions. The results indicate a weakening of the Ni–O interactions at the interface, in favour of a change of the Zr–O coordination to adopt configurations closer to the stable low temperature phases.

Keywords: Composites; Defects; Electronic properties; Interfaces; ZrO_2

1. Introduction

Cubic zirconia (c-ZrO_2) is one of the most widely applied ceramic materials in industry. The crystal structure is CaF_2, with an unit cell consisting of an fcc cube of Zr atoms, each one coordinated to eight O atoms located in the diagonals of the cubes at equal distances to all neighbouring Zr (2.20 Å).[1] Though this structure is stable only above 2370 °C, it can be stabilized at room temperature inserting dopants such as the oxides of Y, Ca, or Mg, which create O vacancies in the ideal cubic structure. In addition there exist two low temperature phases of ZrO_2. Tetragonal zirconia (t-ZrO_2), stable over 1180 °C, shows two kind of Zr–O distances, around 2.40 and 2.05 Å.[2] Below 1180 °C the stable structure is the monoclinic (m-ZrO_2), where each Zr atom is 7-fold coordinated to O in a complex unit cell that contains three ranges of interatomic distances: below 2.10 Å, around 2.17 Å and over 2.25 Å.[3]

Most technological applications of ZrO_2 are based on composites formed introducing metallic particles into the ceramic matrix, in order to improve the electrical and mechanical properties. Among them, Ni/ZrO_2 cermets offer the advantage of the small lattice mismatch between both materials. However, it has been observed experimentally that an embrittlement of the mechanical properties occur in yttria-stabilized ZrO_2 after addition of Ni particles. This has been attributed to a weak interaction at the metal/ceramic interface on the basis of qualitative arguments.[4] A more rigorous study of the bonds at the atomic level is thus required, to understand the microscopic mechanisms that govern the adhesion between both materials.

In this paper we examine the electronic bonding properties of the interface between c-ZrO_2(001) and fcc Ni(001) from a fundamental point of view. To our knowledge, there are only two previous ab-initio studies of the ideal ZrO_2/Ni interface.[5,6] Ref. 5 considers the adhesion of 1–3 c-ZrO_2(111) layers on a Ni(111) substrate of three layers, concluding that it is weakened as we go from the monolayer limit to thicker slabs. In Ref. 6 we analyze the ideal Ni(001)/c-ZrO_2(001) interface in the absence of defects, to find that strong metal/ceramic bonds can be obtained between perfect surfaces. Continuing this analysis, here we focus on the role of defects in the adhesion between both materials, considering the effect of an O vacancy in the interface. Our study is based on ab-initio calculations of the electronic properties of the stable structure, determined self-consistently after full relaxation of the atomic positions.

2. Model and method

All calculations have been performed with the SIESTA code, [7] based on the standard Kohn–Sham self-consistent density functional method in the generalized gradient approximation (GGA). [8] The core electrons are replaced by norm-conserving pseudopotentials. A linear combination of localized numerical atomic orbitals has been used as basis set, allowing arbitraty angular momenta, mutiple-zeta, polarized orbitals. In the case of

* Corresponding author. Tel.: +34-91-334-9097; fax: +34-91-372-06-23.
E-mail address: mcarmen@icmm.csic.es (M.C. Muñoz).

0955-2219/03/$ - see front matter © 2003 Elsevier Ltd. All rights reserved.
doi:10.1016/S0955-2219(03)00284-X

Ni, we chose double-zeta (DZ) basis for the s and d AOs plus a single-zeta (SZ) p AO. The same type of basis set was used for Zr, whereas for O we employed DZ s and p AOs plus a SZ d AO. The Ni–ZrO_2 interface is modelled within a supercell approach, adhering two slabs periodic in two dimensions (2D) of three layers of fcc Ni(001) and three layers of c-ZrO_2(001) (each layer containing two atomic planes, one of Zr and one of O). Periodic boundary conditions are imposed in the perpendicular direction of the slab, normal to the interface plane. This (3/3) supercell, with the atomic positions referred to the final equilibrium values, is depicted in Fig. 1. The lattices of Ni(001) and ZrO_2(001) have been matched at the interface plane aligning the Ni[100] direction to the [110] direction of ZrO_2, and assuming a slight distortion of the fcc Ni lattice to adopt the in-plane ZrO_2 lattice constant. Among the different positions of the Ni atoms relative to the 2D-unit cell of ZrO_2, we will only consider here that corresponding to the equilibrium structure of the ideal interface, with Ni 2-fold coordinated to oxygen.[6] In spite of the reduced thickness, the results reproduce within less than 3% those obtained for thicker (5/5) slabs in the absence of O defects, concerning the Ni–O bond length and the charges and magnetic moments at both the interface and the inner bulk-like layers.

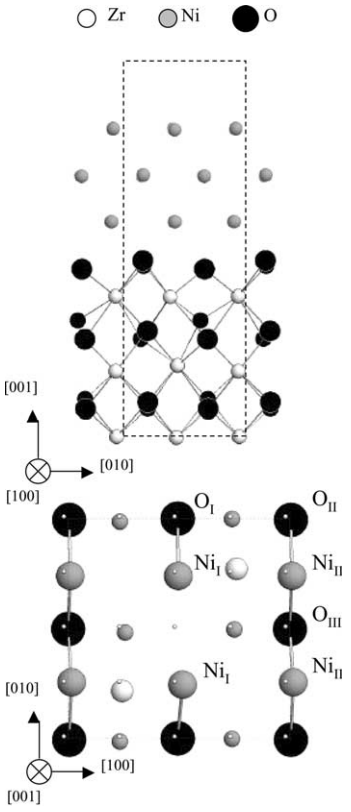

Fig. 1. Side view of the slab supercell (up) and its projection onto the plane of the interface (down). On the lower picture, the size of the atoms is scaled with respect to their distance to the interface, while the small dots on top indicate the starting ideal atomic positions at the non-relaxed lattice. The 2D unit cell, centered in the vacancy site, is delimited by a dashed line.

An O vacancy is introduced in the Ni–O interface removing one out of four O atoms, as indicated in Fig. 1. The 2D symmetry is consequently lowered with respect to the ideal interface, the resulting unit cell being enlarged. The equilibrium structure is obtained self-consistently after relaxation of all atomic positions of the slab in the three directions. The final atomic forces are less than 0.06 eV/Å for all atoms of the slab.

3. Results

Before addressing the results for the case with O vacancies, we will briefly summarize those corresponding to the ideal Ni(001)/c-ZrO_2(001) interface in the absence of defects. Slight relaxations of the atomic positions can be found, leading to bulk-like interatomic distances at the ceramic and metal slabs, and values of d(Ni–O) = 1.99 Å at the O/Ni interface. The nature of the interactions is governed by the electron transfer from Ni to O, which results in ionic bonding.

When an O vacancy is introduced, a deep restructuring occurs. The existence of a vacancy breaks the original *pmm* symmetry of the system. This leads to large displacements of all atoms along the three directions. The atomic positions of the ideal and relaxed structures are shown in Fig. 1. Two types of Ni sites can be distinguished at the interface: those nearest neighbours to the vacancy (Ni_I), which are 1-fold coordinated to oxygen (O_I), and the 2-fold O-coordinated Ni_{II} atoms. The Ni–O bond distances are presented in Table 1. Ni_I shows a slightly enlarged Ni–O bond length with respect to the ideal interface, while the Ni_{II} atoms come closer to one of the O neighbours, O_{II}, at the cost of increasing their distance to the other, O_{III}. Thus, on average the Ni atoms tend to be farther from O than in the absence of vacancies, though locally some strengthened Ni–O bonds are found. The above picture is confirmed through the analysis of the total charges and moments, shown in Table 2. The presence of the vacancy leads to two types of Ni net charges, corresponding to the two types of Ni sites. The Ni_I atoms transfer charge only to the adjacent O_I, keeping values close to the bulk both

Table 1
Interatomic distances and bonding overlap populations (BOP) for the different Ni–O pairs at the interface. The corresponding values of the ideal interface without vacancies are also given

	d (Å)	BOP
Ni_I–O_I	2.04	1.20
Ni_{II}–O_{II}	1.95	1.39
Ni_{II}–O_{III}	2.14	0.87
Ideal	1.99	1.29

for the charge and magnetic moment. On the contrary, the Ni_{II} values are similar to those corresponding to the ideal interface. Since all Oxygen atoms are 2-fold coordinated to Ni, their average charge is similar to the ideal case, though they show lower magnetic moments. This decreased spin polarization may be a consequence of the global reduction of the Ni magnetic moments.

In Fig. 2 the local density of states (LDOS) projected at the interface atoms is presented, together with the corresponding curves for the ideal case. All Ni atoms in the figure show induced interface features, which consist in an enhancement of the spin exchange splitting and the broadening of the minority band. However, at the interface with vacancies, both effects are more pronounced for Ni_{II}, which becomes more similar to the ideal case. Regarding O, intrinsic interface states can be observed in the oxide energy gap (starting approximately at −2.5 eV) for all cases. There are also changes in the bulk band continua, mainly consisting of a large broadening of the DOS. Again these effects are more pronounced for O_{II} and at the interface without vacancies. All the above results seem to indicate that the presence of the vacancy reduces the ionic interaction between Ni and O, which may be a hint of a weakened bonding. However, it may happen that the bond has changed to a more covalent situation. To shed more light to this point, we have analyzed the charge shared by the Ni–O bonds through the bonding overlap populations (BOPs).[9] They are given in Table 1, where they are compared to the values at the interface without vacancies (with only one kind of Ni–O bonds). They reflect that the bonding contribution is directly related to the interatomic distances: the closer the Ni–O pair, the larger the bonding charge. Thus, though the bonding character is stronger for some Ni–O pairs, on the average the net charge sharing for the Ni–O bonds is smaller in the presence of vacancies.

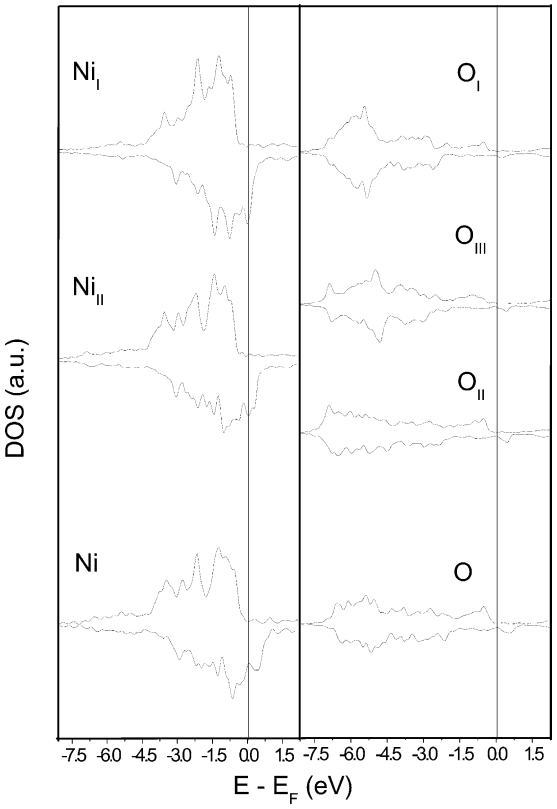

Fig. 2. Spin-resolved DOS of the Ni and O atoms at the interface plane for the cases with and without (lower row) vacancies. For each atom, positive (negative) values of the DOS correspond to the majority (minority) spin.

The existence of oxygen vacancies induces large displacements of the atoms not only at the interface, but across the entire slab. This effect is less pronounced on the Ni side, where the largest shifts from the ideal positions correspond to the interface layer. The in-plane displacements reach maximum values of 0.18 Å, and corrugations of 0.07 Å appear. However, there is no net tendency of distortion around the vacancy site. The main relaxations can be found at the ZrO_2 slab, involving both the Zr and O atoms. They are not only restricted to the planes closer to the vacancy site, but

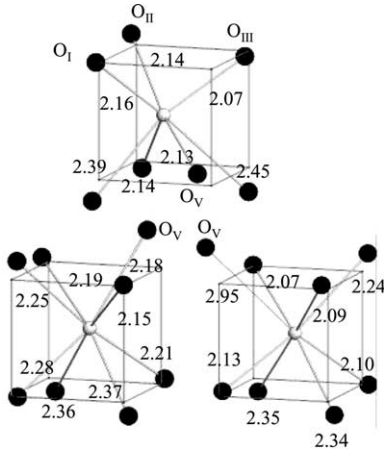

Fig. 3. Zr–O bonding units for the Zr layer closest to the interface (upper) and for the two kinds of Zr atoms at the layer below. Numbers indicate the corresponding bond lengths in Å.

Table 2
Total charges and spin moments of the atoms at the interface (as a reference, the values for fcc bulk Ni and for the atoms at the ideal interface are shown. Units of the moments are μ_B)

	Ni_I	Ni_{II}	Ni_{ideal}	Ni_{bulk}	O_I	O_{II}	O_{III}	O_{ideal}
Q	9.85	9.76	9.74	10.00	6.64	6.65	6.62	6.63
μ	0.68	0.81	0.85	0.66	0.06	0.14	0.09	0.17

extend even four planes below. The largest displacements correspond to the O atom immediately below the vacancy along the normal to the interface (O_V), which shifts from its ideal position by more than 0.35 Å in all directions (0.39 Å towards the vacancy site in Z). A general trend can be extracted after analyzing in detail the resulting interatomic distances. In Fig. 3 we depict the different kinds of Zr–O bonding units encountered in the relaxed slab. Among the Zr atoms, those closest to the vacancy show the largest displacements and both exhibit a 7-fold coordination. The corresponding Zr–O bond distances range from 2.07 to 2.45 Å. Also one of the atoms of the underlying Zr plane exhibits this behaviour, induced by the large movement of O_V. The rest of Zr maintain the 8-fold coordination, although the distribution of Zr–O distances resembles the situation of the monoclinic and tetragonal phases, where different distances ranging from 2.05 to ~2.40 Å can be found in the unit cell. Thus, it seems that the presence of the vacancy induces a local redistribution at the ZrO_2 slab, trying to approach bulk configurations which are stable at low temperatures.

Regarding the net charge at the ZrO_2 slab, while the 8-fold coordinated Zr atoms maintain bulk-like values of 2.48, those 7-fold coordinated experience a reduction in the amount of charge transfer, which results in a maximum charge of 2.59 for the Zr closest to the interface. On the other hand, the analysis of the bonds strength reveals a global enhancement of the bonding character with respect to the ideal interface, even if the ionic charge is smaller. This can be confirmed through the average BOP/bond, which sums up to 0.144 for a representative Zr–O bonding unit against the average value of 0.128 for the case with no vacancies. Thus, it can be concluded that the Ni–O interaction is weakened in favour of the Zr–O bonds at the interface.

4. Conclusions

The presence of an O vacancy at the Ni–O interface between Ni(001) and c-ZrO2(001) sligthly reduces the ionic Ni–O interaction, and on average decreases the bonding character. It also induces a strong restructuring of the atomic positions, mainly at the ZrO_2 side. This results in 7-fold coordination of the Zr atoms closer to the interface, in an arrangement resembling the low temperature ZrO_2 phases. In summary, the intraceramic interactions seem to dominate over those at the interface, leading to a weakened bonding character of the Ni–O interaction in favour of strengthened Zr–O bonds.

Acknowledgements

This work has been partially financied by the Spanish DGICyT under contracts BFM2000/1330 and MAT2001-1596. S.G. acknowledges financial support from the Comunidad Autónoma de Madrid.

References

1. Stefanovich, E. V., Shluger, A. L. and Catlow, C. R. A., *Phys. Rev. B*, 1994, **49**, 11560.
2. Aldebert, P. and Travers, J.P., *J. Am. Ceram. Soc*., 1985, **68**, 34; Stevens, R., *Zirconia and Zirconia Ceramics*. Magnesium Elektron Ltd., 1985.
3. Smith, D.K. and Newkirk, H.W., *Acta Crystallogr*., 1965, **18**, 983;
   Foster, A.S., Sulimov, V.B., Lopez, Gejo, F., Shluger, A.L., Nieminen, R.M.*Phys. Rev. B*, 2001, **64**, 224108.
4. López-Esteban, S., Bartolomé, J. F. and Moya, J. S., *J. Mater. Res*., 2002, **17**, 1592.
5. Christensen, A. and Carter, E. A., *J. Chem. Phys*., 2001, **114**, 5816.
6. Beltrán, J. I., Gallego, S., Cerdá, J., Moya, J. S., Muñoz, M.C., Phys. Rev. Lett., in press.
7. Soler, J. M., Artacho, E., Gale, J. D., García, A., Junquera, J., Ordejón, P. and Sánchez-Portal, D., *J. Phys.: Condens. Matter*, 2002, **14**, 274.
8. Perdew, J. P., Chevary, J. A., Vosko, S. H., Jackson, K. A., Pederson, M. R., Singh, D. J. and Fiolhais, C., *Phys. Rev. B*, 1992, **46**, 6671.
9. Ammeter, J. H., Bürgi, H. B., Thibeault, J. C. and Hoffmann, R., *J. Am. Chem. Soc*., 1978, **100**, 3687.